Anal. Chem. **2006,** *78,* 3265−3270

Virus Electrodes for Universal Biodetection

Li-Mei C. Yang, Phillip Y. Tam, Benjamin J. Murray, Theresa M. McIntire, Cathie M. Overstreet, Gregory A. Weiss,* and Reginald M. Penner*

Department of Chemistry, University of California, Irvine, California 92697-2025

A dense virus layer, readily tailored for recognition of essentially any biomarker, was covalently attached to a gold electrode surface through a self-assembled monolayer. The resistance of this "virus electrode", Z_{Re}, measured in the frequency range from 2 to 500 kHz in a salt-based pH 7.2 buffer, increased when the phage particles selectively bound either an antibody or prostate-specific membrane antigen (PSMA), a biomarker for prostate cancer. In contrast to prior results, we show the capacitive impedence of the virus electrode, Z_{Im}, is both a noisier and a less sensitive indicator of this binding compared to Z_{Re}. The specificity of antibody and PSMA binding, and the absence of nonspecific binding to the virus electrode, was confirmed using quartz crystal microbalance gravimetry.

With up to 10^{12} unique members, phage-displayed libraries provide a vast pool of candidate receptors to essentially any target, including small molecules, DNA, RNA, and proteins.[1,2] Despite the tremendous potential of phage-displayed libraries for universal molecular recognition, the technique has found only limited application in biosensors. Detecting molecular recognition between phage and target until now has focused on a "sandwich assay" scheme involving the detection of phage binding to immobilized target using quartz crystal microbalance,[3−7] microelectrode arrays,[8] nanowire field-effect transistors,[9] bead-based electrochemical immunoassay,[10] electric DNA chips, [11] infection of different bacteria,[12,13] or fluoroimmunoassays.[14,15] An unexplored and potentially more attractive approach is to immobilize the phage on the sensor surface and directly detect the binding of analyte. This approach offers the most straightforward strategy for real-time sensing of analyte since the phage can be permanently affixed to a surface and continually exposed to the solution. In terms of the potential for achieving miniaturization and a rapid response time, it would be most desirable if the binding of analyte molecules generated an electrical signal that was directly measurable at the virus electrode.

Here we describe such a biosensor (Figure 1) based on the covalent attachment of virus particles to a gold electrode surface (Figure 1b). The virus employed in this study, a bacteriophage called M13, can selectively and simultaneously bind two biomolecules: an antibody (henceforth p-Ab) and prostate-specific membrane antigen (PSMA). This binding activity was engineered through phage display. A negative control antibody (henceforth n-Ab) was used to evaluate nonspecific binding and biosensor selectivity (Figure 1c). The surface chemistry employed to prepare virus electrodes was optimized to permit stable measurements in concentrated buffer solutions to be conducted for up to 6 h. Using electrochemical impedance spectroscopy, we demonstrate high signal-to-noise ratios (S/N > 10) for detection of binding and recognition in the resistive component of the impedance, Z_{Re}, at relatively high frequencies from 2 to 500 kHz (Figure 1d) for concentrations down to 100 nM. This strategy stands in contrast to previous electrochemical biosensors, which have employed measurements of the capacitive impedance (Z_{Im}) at much lower frequencies (<100 Hz).[16−19]

EXPERIMENTAL SECTION

Materials. All chemicals and solvents (>99% purity) were purchased from Fisher or Merck and used as received, unless noted. DMF and ethanol were dried with 4-Å molecular sieves obtained from Alfa. The anti-M13 antibody (p-Ab) was purchased from Amersham Biosciences, and the anti-Flag M2 (n-Ab) was purchased from Sigma. Nanopure water (resistance ∼18 MΩ·cm, Barnstead Inc.) was used in all experiments. PSMA was a generous gift from Pamela Bjorkman, Melanie Bennett Brewer

* Corresponding authors. E-mail: rmpenner@uci.edu; gweiss@uci.edu.

(1) Smith, G. P. *Science* **1985**, *228*, 1315−1317.
(2) Smothers, J. F.; Henikoff, S.; Carter, P. *Science* **2002**, *298*, 621−622.
(3) Decker, J.; Weinberger, K.; Prohaska, E.; Hauck, S.; Kosslinger, C.; Wolf, H.; Hengerer, A. *J. Immunol. Methods* **2000**, *233*, 159−165.
(4) Dultsev, F. N.; Speight, R. E.; Fiorini, M. T.; Blackburn, J. M.; Abell, C.; Ostanin, V. P.; Klenerman, D. *Anal. Chem.* **2001**, *73*, 3935−3939.
(5) Hengerer, A.; Decker, J.; Prohaska, E.; Hauck, S.; Kosslinger, C.; Wolf, H. *Biosens. Bioelectron.* **1999**, *14*, 139−144.
(6) Hengerer, A.; Kosslinger, C.; Decker, J.; Hauck, S.; Queitsch, I.; Wolf, H.; Dubel, S. *Biotechniques* **1999**, *26*, 956−964.
(7) Uttenthaler, E.; Schraml, M.; Mandel, J.; Drost, S. *Biosens. Bioelectron.* **2001**, *16*, 735−743.
(8) Dill, K.; Montgomery, D. D.; Ghindilis, A. L.; Schwarzkopf, K. R.; Ragsdale, S. R.; Oleinikov, A. V. *Biosens. Bioelectron.* **2004**, *20*, 736−742.
(9) Patolsky, F.; Zheng, G.; Hayden, O.; Lakadamyali, M.; Zhuang, X.; Lieber, C. M. *Proc. Natl. Acad. Sci. U.S.A.* **2004**, *101*, 14017−14022.
(10) Thomas, J. H.; Kim, S. K.; Hesketh, P. J.; Halsall, H. B.; Heineman, W. R. *Anal. Chem.* **2004**, *76*, 2700−2707.
(11) Gabig-Ciminska, M.; Los, M.; Holmgren, A.; Albers, J.; Czyz, A.; Hintsche, R.; Wegrzyn, G.; Enfors, S. O. *Anal. Biochem.* **2004**, *324*, 84−91.
(12) Neufeld, T.; Mittelman, A. S.; Buchner, V.; Rishpon, J. *Anal. Chem.* **2005**, *77*, 652−657.
(13) Neufeld, T.; Schwartz-Mittelmann, A.; Biran, D.; Ron, E. Z.; Rishpon, J. *Anal. Chem.* **2003**, *75*, 580−585.
(14) Goldman, E. R.; Pazirandeh, M. P.; Charles, P. T.; Balighian, E. D.; Anderson, G. P. *Anal. Chim. Acta* **2002**, *457*, 13−19.
(15) Goldman, E. R.; Pazirandeh, M. P.; Mauro, J. M.; King, K. D.; Frey, J. C.; Anderson, G. P. *J. Mol. Recognit.* **2000**, *13*, 382−387.
(16) Corry, B.; Uilk, J.; Crawley, C. *Anal. Chim, Acta* **2003**, *496*, 103−116.
(17) Desilva, M. S.; Zhang, Y.; Hesketh, P. J.; Maclay, G. J.; Gendel, S. M.; Stetter, J. R. *Biosens. Bioelectron.* **1995**, *10*, 675−682.
(18) Lasseter, T. L.; Cai, W.; Hamers, R. J. *Analyst* **2004**, *129*, 3−8.
(19) Rickert, J.; Gopel, W.; Beck, W.; Jung, G.; Heiduschka, P. *Biosens. Bioelectron.* **1996**, *11*, 757−768.

10.1021/ac052287u CCC: $33.50
Published on Web 04/06/2006

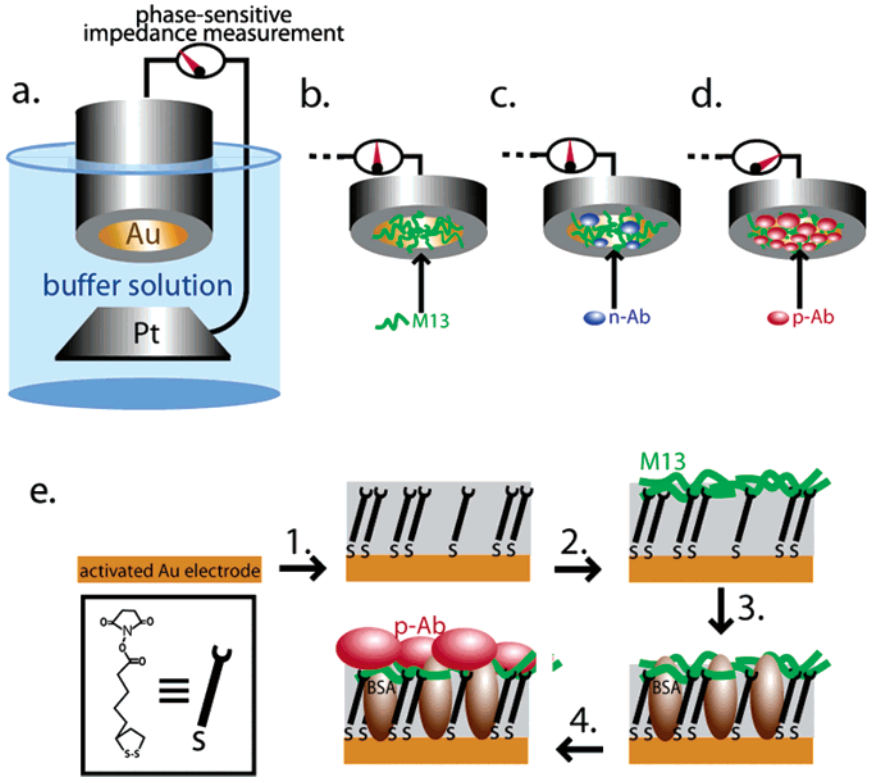

Figure 1. Virus electrode, 3-mm-diameter gold disk electrode onto which engineered M13 phage particles are covalently attached according to the steps 1−3 shown in (e). The state of this electrode was determined by measuring its resistive impedance, Z_{Re}, at high frequency (2−500 kHz) versus a large area platinum electrode immersed in the same salt-based buffer solution. Prior to the attachment of phage particles (a), Z_{Re} of this system, at all frequencies, was relatively low. (b) A dense virus layer was then covalently bonded to the gold surface according to the steps labeled 1−3 shown in (e). This produces a dense phage layer that completely electrically insulates the gold surface from contact with the buffer solution. (c) Exposure of this virus electrode to a "negative" antibody (n-Ab, blue) causes no change to either the imaginary component of impedance, Z_{Im} or to Z_{Re}. (d) Exposure to a "positive" antibody (p-Ab, red) that is selectively recognized and bound by the phage causes a significant increase in the high-frequency Z_{Re}, but little change in Z_{Im} (at any frequency). Separately, QCM measurements measure the uptake of the two antibodies by the virus electrode. (e) Schematic view of the step involved in the preparation of a virus electrode investigated here. Step 1. An electrochemically activated gold electrode was exposed to thioctyl NHS ester to form a thiol−Au bonded SAM, Step 2. M13 phage was covalently tethered to the self-assembled monolayer, through formation of amide bonds between free amines on the phage and the activated carboxylate, Step 3. Gaps in the monolayer and unreacted NHS esters were capped with BSA, Step 4. The virus electrode is ready to be used for analyses.

(HHMI, Caltech), William Ernst, and Gary Fuji (Molecular Express). Phosphate-buffered fluoride buffer (PBF: 5.7 mM PO_4, 140 mM NaF, pH 7.2) was filter sterilized through a 0.22-μm pore size membrane (Corning). For the wash buffer, 0.06% BSA and 0.035% Tween-20 (Sigma) were added to PBF. BSA (0.2%) in phosphate-buffered sodium fluoride (pH 7.2) solution was used for blocking.

Virus Electrode Construction. Circular gold electrodes (3-mm diameter) were polished with 1- and 0.25-μm diamond compound (Ted Pella) on microcloth (Buehler) and sonicated three times in Nanopure water for 3 min. Freshly prepared electrodes were rinsed with Nanopure water, dried with N_2, and incubated for at least 18 h in a solution of *N*-hydroxysuccinimide thioctic ester (NHS-TE, 16.5 mM) dissolved in DMF. The NHS-TE modified electrode was stored in a desiccator. Phage with specific binding affinity for PSMA were selected from phage-displayed peptide libraries using previously described techniques.[21] The amino acid sequence of the PSMA-specific peptide was CALCEFLG. For reaction with the phage, a NHS-TE-modified electrode was incubated in a phage solution (300 μL, 16 nM) and shaken for 1 h by orbital shaker. Virus electrodes were rinsed 5 min with wash buffer and then 5 min with PBF. Virus electrodes were dipped in 300 μL of 0.2% BSA solution and shaken another 40 min. The virus/BSA-modified electrodes were rinsed for 5 min with Tween-20/PBF buffer and then 5 min with wash buffer.

Measurements with Virus Electrodes. For biosensor experiments, n-Ab, p-Ab, or PSMA (final concentration of 0.583 μM or as indicated) was diluted in wash buffer before the measurement. The virus electrode was immersed in the n-Ab, p-Ab, or PSMA solution with shaking for 1 h. The electrode was rinsed with wash buffer, before immersion for 1 min in wash buffer for the following impedance measurement. All impedance measurements were carried out using a Parstat 2263 potentiostat (Princeton Applied Research Inc.). These measurements were carried out at rest potential of the virus electrode and involved the application of an ac voltage with an amplitude of 10 mV over the frequency range from 1 MHz to 0.1 Hz. All cyclic voltammetry measurements were carried out in aqueous PBF using a saturated calomel electrode (SCE) reference electrode and a platinum counter electrode. A

(20) Widrig, C. A.; Chung, C.; Porter, M. D. *J. Electroanal. Chem.* **1991**, *310*, 335−359.
(21) Murase, K.; Morrison, K. L.; Tam, P. Y.; Stafford, R. L.; Jurnak, F.; Weiss, G. A. *Chem. Biol.* **2003**, *10*, 161−168.

voltage scan rate of 20 mV s^{-1} was used for all cyclic voltammograms.

QCM Measurements. Au/Ti quartz disks (1-in. diameter) were prepared as described for the virus electrodes except that a fresh gold layer was first electrodeposited on the gold-covered quartz oscillator obtained from the manufacturer (Stanford Research Systems) by applying +0.7 V versus SCE for 200 s in 10 mM $AuCl_3$ solution (pH 1). After gold deposition, the same procedure was employed for the attachment of viruses. This electrode was then placed in a flow cell that provided for a radially symmetric delivery of solution to the circular quartz crystal microbalance (QCM) electrode surface. Mass measurements at this surface were made using using a QCM 200 (quartz crystal microbalance digital controller, 5-MHz crystal oscillator, Stanford Research Systems) using a flow rate of 10 μL min^{-1} from a syringe pump (Kd Scientific Inc.).

AFM Analysis. Intermittent contact mode atomic force microscopy (AFM) images were obtained in air at ambient pressure and humidity using a Park Scientific Instruments AutoProbe CP Research (now Veeco, Santa Barbara, CA) scanning probe microscope. The piezoelectric scanner was calibrated using a 1.0-μm grating in the *xy* directions and in the *z* direction using several conventional height standards. The tips were silicon (Ultrasharp cantilevers, model NSC11, MikroMasch). Topographs were obtained as 256 × 256 pixels and were flattened line-by-line and analyzed using AutoProbe image processing software supplied by the manufacturer.

Fluorescence Analysis. Interdigitated electrodes with 2-μm gaps were made by photolithography in a clean room. The surface modification was similar to the preparation of the virus electrodes, except assembly took place in a PDMS flow cell with a 0.3-mm-wide and 0.8-mm-long channel. Fluorescein labeled anti-M13 antibody was added by syringe pump at the rate of 10 μL/min before rinsing with PBF−Tween and PBF solution for 10 min each. Optical micrographs of the electrode were acquired using an Axioskop2 MAT microscope (Carl Zeiss Micromaging Inc.) equipped with an appropriate filter and Nikon Coolpix 5000 digital camera.

RESULTS AND DISCUSSION

The biosensor consisted of a gold electrode covalently modified by M13 phage, which bind an anti-M13 monoclonal antibody (p-Ab). For recognition of the prostate cancer marker, PSMA, phage with high affinity for PSMA were isolated from selections of a ~5 × 10^{11} diversity peptide library. This PSMA-phage binds both PSMA and p-Ab and, like M13 phage, fails to bind negative control antibody (anti-Flag M2, anti-His tag monoclonal Ab). Phage and antibody were attached and measured in PBF−Tween−BSA solutions, with the exception of the QCM experiments that omitted BSA to reduce background. This buffer provides a realistic assessment of the potential for this device to perform physiological measurements as it includes a high salt concentration (I > 140 mM) and pH 7.2.

Preparation of a pinhole-free, covalent virus surface proved critical for reliable electrochemical measurements. The gold surface was first polished and then activated by briefly electrodepositing a small amount of fresh gold. As shown schematically in Figure 1e, phage were anchored to the gold via a self-assembled monolayer (SAM) of thioctyl NHS ester. This SAM required ~18 h to assemble from a dry DMF solution of the NHS-activated ester. After the reaction of this SAM with the phage, a dense, electrically resistive covalent virus layer was obtained.

Imaged by AFM, the clean gold surface was characterized by a rms roughness of <1 nm with 10-μm-diameter gold grains delineated by grain boundaries (Figure 2a). After covalent virus modification (Figure 1e, step 2), NC-AFM imaging shows a striated surface with a roughness of 2−3 nm (Figure 2b). Since individual M13 phage particles are ~6−8 nm in diameter and ~1 μm in length, the striations observed in Figure 2b are consistent with the presence of aligned bundles of phage M13 particles (red lines) on the gold surface. In conjunction with BSA adsorbed in step 3, this covalent virus layer sharply increased the resistance of the electrode surface (Figure 2c) with the largest increase observed at lower frequencies.

The covalent virus surface layer, after exposure to BSA, was dense enough to completely suppress electrochemical signatures of the underlying gold surface (Figure 2d). The cyclic voltammogram for a bare gold electrode in PBF buffer (Figure 2c, gold trace) shows three electrochemical reactions: reversible oxidation of the gold (at 0.5 V), reduction of the resultant gold oxide (at 0.2 V), and reduction of H^+ to form H_2 (at 0.0 V). After covalent virus modification and BSA/p-Ab treatment, none of these three reactions is observed (Figure 2d, green trace) indicating that the gold electrode is insulated from direct contact with the electrolyte solution. If the potential of this electrode is scanned repeatedly to +1.0 V, the SAM is oxidatively desorbed,[20] thereby releasing the virus and p-Ab from the gold surface. As the SAM desorption proceeds over the course of 10 voltammetric scans (black CVs), current peaks that are characteristic of bare gold emerge. The biosensor selectivity for p-Ab versus n-Ab and PSMA that we demonstrate next required covalent virus surfaces with strong passivation of the gold surface as seen here.

To guide development of the virus electrode, we used two independent methods to evaluate the functioning of the covalent virus surface. First, QCM gravimetry permitted mass changes at the covalent virus surface to be directly measured during the exposure of these surfaces to p-Ab and n-Ab (Figure 3a). QCM measurements revealed that virus electrodes rapidly and irreversibly bind p-Ab but do not bind n-Ab to any measurable extent. Omission of phage (step 2), followed by addition of buffer and BSA, resulted in a surface that was incapable of binding fluorescently labeled p-Ab (Figure 3c). As expected, the covalent virus surface recognized and bound the fluorescently labeled p-Ab (Figure 3d).

Electrochemical impedance spectroscopy was used to evaluate performance by the virus electrode in response to n-Ab, PSMA, and p-Ab (Figure 4). These experiments explored two modes of detection. First, the virus electrode was exposed to analyte for 1 h, rinsed with wash buffer, and then transferred to wash buffer for impedance measurement. In Figure 4, signal is defined as the change in impedance—either capacitive, ΔZ_{Im} (Figure 4A), or resistive, ΔZ_{Re} (Figure 4b)—relative to the initial impedance of the covalent virus surface, following BSA treatment. In the frequency range from 100 Hz to dc, the magnitude of both ΔZ_{Im} and ΔZ_{Re} increased exponentially with the reduction in frequency. The large signal amplitude seen at very low frequencies has also been seen in previous studies of electrochemical biosensors and

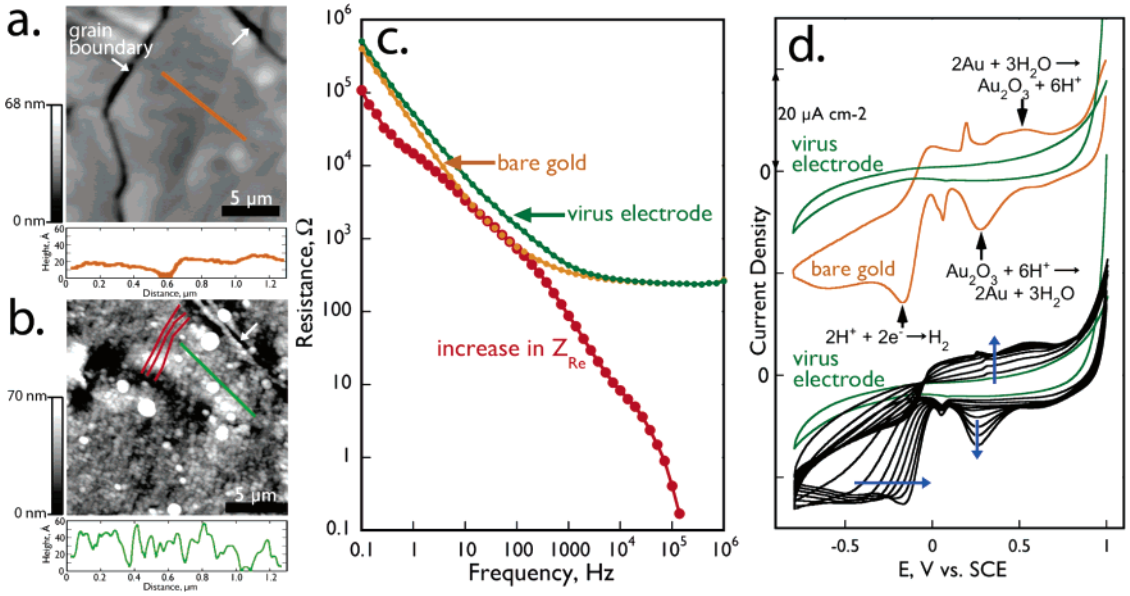

Figure 2. (a) AFM image of a flame-annealed gold surface on quartz. (b) AFM image of a similar gold electrode after covalent attachment of phage (Figure 1e, step 2). The striations seen in this image of a dense phage layer are assigned to 30-nm-diameter bundles of M13 phage particles (indicated in red). (c) Plot of the electrode resistance, Z_{Re}, as a function of frequency for a bare gold electrode before (gold) and after (green) the covalent attachment of M13 phage and exposure of this surface to BSA (Figure 1e, step 3). An increase in resistance, relative to clean gold results from this layer of phage and BSA (red). (d) Cyclic voltammograms at 20 mV s^{-1} for a clean gold electrode (top, gold trace) in PBF and for a phage-covered biosensor (green traces) following experiments to assess the response to n-Ab and p-Ab lasting >8−10 h in flowing buffer. Reactions characteristic of exposed gold—including the reduction of protons (at 0.0 V) and the oxidation and reduction of the gold surface (at 0.2 and −0.55 V, respectively)—were suppressed by the covalent virus layer. This layer could be removed, gradually, by scanning (blue arrows) the potential of this electrode to +1.0 V vs SCE revealing the characteristic voltammetric features of the underlying gold surface.

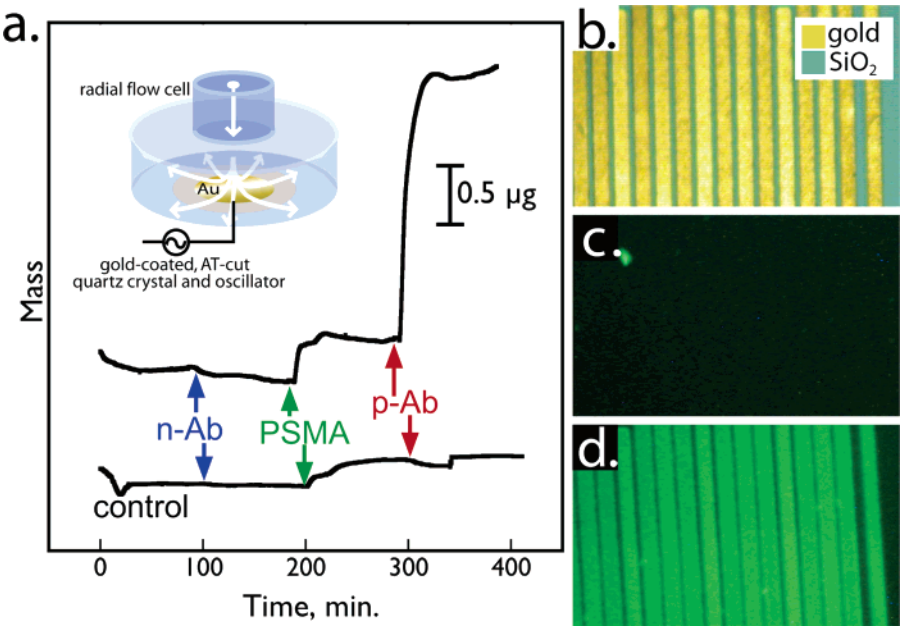

Figure 3. (a) Flow cell-based QCM measurements of mass versus time showing the exposure of a virus electrode to n-Ab, PSMA, and p-Ab demonstrating selective binding of p-Ab and PSMA and the absence of nonselective binding to n-Ab. Shown are the response of a virus electrode prepared according to the steps shown in Figure 1e (top trace), and a second electrode on which no virus was attached, corresponding to omission of step 2 in Figure 1e. (b) Photomicrograph of a gold electrodes patterned on silicon after the formation of a covalent virus surface. (c) Fluorescence micrograph of similarly patterned gold electrodes exposed to thioctyl NHS ester, followed by consecutive incubation in buffer, BSA, and then fluorescein-labeled p-Ab. In this experiment, which omits the M13 phage, no binding to the electrode is observed. (d) Fluorescence micrograph after the attachment of M13 phage to the thioctyl SAM and binding of fluorescein-labeled p-Ab.

this has provided the rational for employing frequencies below 1 Hz in these devices.[18−20] However, we find that the measurement-to-measurement variability of ΔZ_{Im} and ΔZ_{Re}, as measured by the standard deviation obtained for replicate measurements, $\sigma_{\Delta Z}$ (plotted as error bars in Figure 4a,b), increased in parallel with ΔZ for both ΔZ_{Im} and ΔZ_{Re}. Thus, low frequencies provide a large signal, but a proportionally larger noise background. Between 2 and 500 kHz, ΔZ_{Im} becomes small (Figure 4a), but ΔZ_{Re} is readily

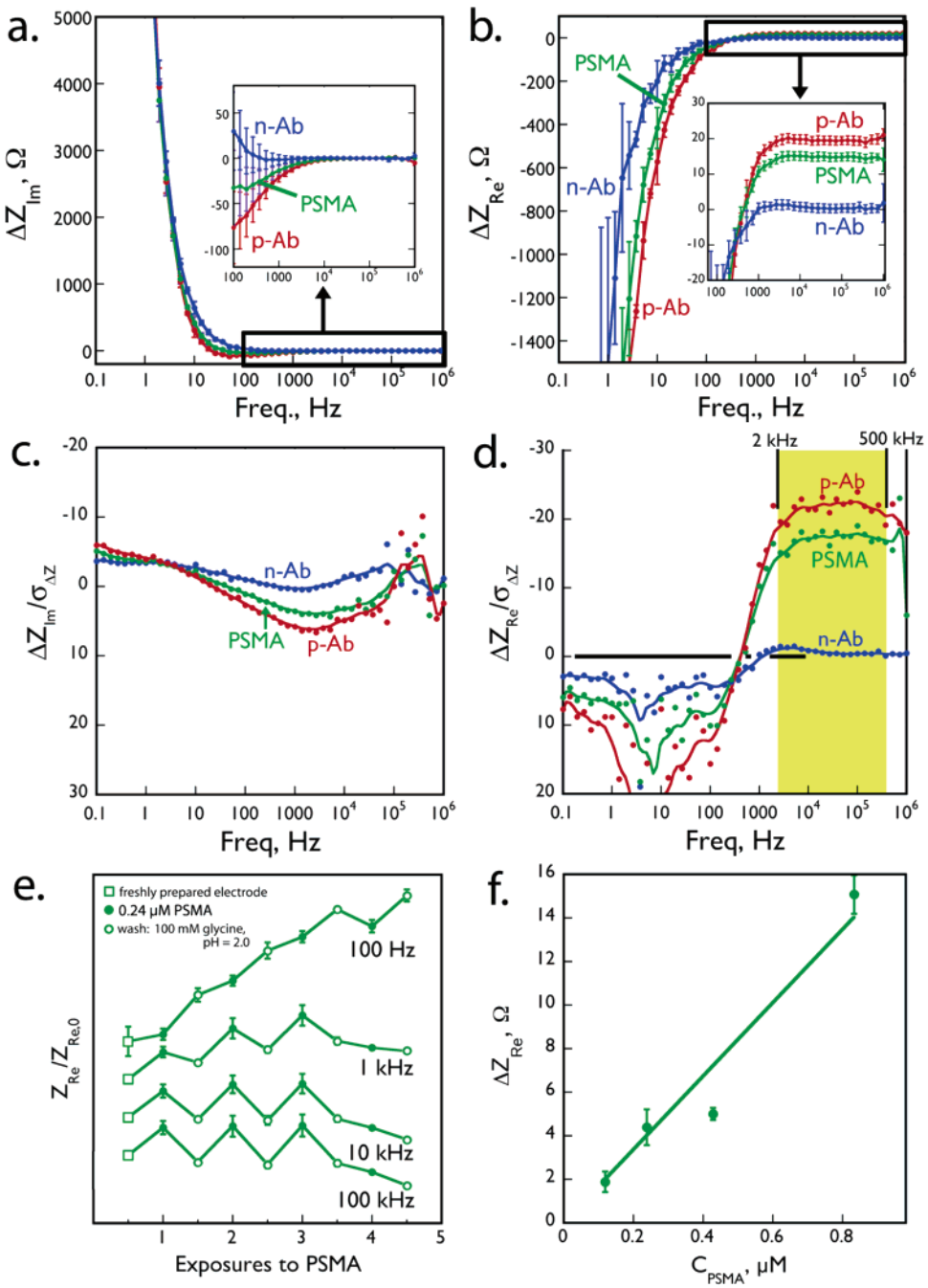

Figure 4. (a,b) Electrochemical impedance spectroscopy measured at a 3-mm-diameter gold disk biosensor. This covalent virus electrode was exposed consecutively to n-Ab (blue), PSMA (green), and p-Ab (red). In a real-time measurement, the change in Z_{Im} (ΔZ_{Im}, a) and Z_{Re} (ΔZ_{Re}, b) during exposure to analyte was recorded. The magnitude of ΔZ increased dramatically with decreasing frequency for both real and imaginary components of the impedance, but the measurement-to-measurement variability of ΔZ ($\sigma_{\Delta Z}$, red trace, $N = 3$) increased in parallel with ΔZ. (c,d) S/N ratio, defined as $\Delta Z/\sigma_{\Delta Z}$, plotted as a function of frequency. S/N above 10 is not observed at any frequency for ΔZ_{Im} (C) but relatively high S/N is observed for both PSMA (S/N $\approx$ 16) and p-Ab (S/N $\approx$ 20) over a broad range of frequencies for ΔZ_{Re} from 2 to 500 kHz. Error bars in figures depict the standard deviation. (e) Measurements of Z_{Re} at four frequencies, as indicated, after exposures to 0.24 μM PSMA (●) and after rinsing with aqueous 100 mM glycine, pH 2.0 (○). The resistance of the rinsed state matched that seen for the freshly prepared virus electrode (□). Clean modulation between a high-resistance "bound state" and a low-resistance "rinsed state" was seen only at 10 and 100 kHz. (f) Calibration curve for PSMA detection by virus electrodes prepared as described previously. Measurement of ΔZ_{Re} provides a linear response to variable concentrations of PSMA. Each data point represents the average value obtained from measurements with four identically prepared virus electrodes.

measurable with positive signal for both p-Ab and PSMA and near zero signal for n-Ab (Figure 4b). The positive value of ΔZ_{Re} over this frequency range means that the analyte-bound state of the virus electrode has a higher resistance than the initial state of the electrode before exposure to analyte. This higher resistance may derive from the formation of a bound analyte layer atop the

virus electrode. These bound analyte molecules can both displace electrolyte and impede ion transport to the electrode surface by physically blocking it.

The data of Figure 4a,b suggest that the ratio between ΔZ and $\sigma_{\Delta Z}$ at each frequency provides a better figure of merit than ΔZ. When $\Delta Z/\sigma_{\Delta Z}$, the "signal-to-noise ratio", is plotted versus frequency for both capacitive and resistive channels (Figure 4c,d, respectively), it is apparent that the highest values are obtained in the resistive channel within the frequency range from 2 to 500 kHz. Here, $\Delta Z_{Re}/\sigma_{\Delta Z} = 16$ for PSMA to 20 for p-Ab (Figure 4c,d). Furthermore, measured $\Delta Z_{Re}/\sigma_{\Delta Z}$ values remained virtually invariant over this frequency range.

This conclusion is reinforced by the experiment shown in Figure 4e, which involved measuring the frequency-dependent value of Z_{Re} as a virus electrode was first exposed to PSMA and then subsequently rinsed to release PSMA from the sensor surface. Only at 10 and 100 kHz is the impedance of the freshly prepared virus electrode recovered after this rinsing operation. At these frequencies, the resistance of the high Z_{Re} state associated with bound PSMA and the low Z_{Re} state associated with a clean sensor surface are reproduced for three exposure/rinse cycles prior to failure of the sensor upon the fourth exposure to PSMA. Using 10 kHz, the dependence of ΔZ_{Re} on the concentration of PSMA can be measured (Figure 4f). These data permit a limit of detection for PSMA of ~120 nM to be estimated, a value comparable to levels observed in the seminal fluid of healthy men.[21] In addition to the potential for developing virus electrodes for noninvasive cancer diagnostics, the format could provide sensitive, direct assays for biodefense and other applications.

ACKNOWLEDGMENT

Dr. Erich C. Walter is acknowledged for valuable consultations. R.M.P. acknowledges funding support from the National Science Foundation (Grant CHE-0111557) and the Petroleum Research Fund of the American Chemical Society (Grant 40714-AC5). G.A.W. acknowledges funding support from NSF (Grant EF-0404057). We thank Drs. Pamela Bjorkman (HHMI, Caltech), Melanie Bennet Brewer (HHMI, Caltech), Bill Ernst (Molecular Express), and Gary Fuji (Molecular Express) for generously providing PSMA.

Received for review December 28, 2005. Accepted March 3, 2006.

AC052287U